

FRET Fluctuation Spectroscopy: Exploring the Conformational Dynamics of a DNA Hairpin Loop

Mark Ian Wallace, Liming Ying, Shankar Balasubramanian,* and David Klenerman*

The Department of Chemistry, University of Cambridge, Lensfield Road, Cambridge CB2 1EW, U.K.

Received: April 24, 2000; In Final Form: August 24, 2000

The motions of a dye-labeled DNA hairpin loop (Cy5-5'-GGGTT-(A)₃₀-AACCC-3'-TMR) have been investigated through the fluctuations in proximity ratio from fluorescence resonance energy transfer (FRET). We examine three solution conditions: (1) MilliQ water, (2) Tris-EDTA buffer, and (3) Tris-EDTA buffer plus an excess of DNA complementary to the loop sequence, (T)₃₀. Correlations in proximity ratio show submillisecond dynamics. Static heterogeneity is revealed from the distribution of proximity ratio amplitudes. The observed stretched exponential kinetics are consistent with a model based on the transition between two states over a complex energy landscape.

1. Introduction

Single-molecule spectroscopy has emerged as a powerful tool in exploring the static and dynamic properties of biomolecules.^{1–10} In particular, by attaching donor and acceptor fluorophores to a biological molecule, single-molecule fluorescence resonance energy transfer (FRET) provides a method through which conformational dynamics may be probed.^{4,10,11} However, this technique does have limitations, principal of which is the finite number of photons available from each fluorophore. This requires some form of thresholding algorithm to be applied in order to separate bright fluorescent states from the background noise.^{11,12} Consequently, a compromise must be made between the time scale of measurement and the integration over sufficient time to detect the molecular fluorescence with a high signal-to-noise ratio.

The relation between the time scale of the fluctuating process of interest and the time scale of the measurement determines the nature of the observed dynamics.¹³ To date, all single-molecule FRET experiments have probed dynamics on a time scale longer than 1 ms. For many biological processes of interest, this is enough to resolve only the static heterogeneity; dynamic information is more difficult to obtain.

The recent renaissance in fluorescence fluctuation spectroscopy^{14,15,16} points to another method of examining biomolecular motion: Rather than examining the state of a system one molecule at a time, dynamics can also be probed by looking at the fluctuations from a few molecules (typically, < 10).^{17,18} The increase in signal-to-noise ratio given by examining dynamics from a few molecules enables submillisecond dynamics to be resolved. A compromise is also made between the resolution with which the distribution of molecular states is measured and the proportion of molecular states that may be probed.

The two extremes of this balance are the single-molecule and ensemble regimes. By looking at a few molecules, it is possible to collect information from a large fraction of the total population while retaining enough fluctuation information to provide a measure of the dynamic heterogeneity.

There are two possible sources of information in any fluctuation-based experiment: (i) fluctuations in time and (ii) fluctuations in amplitude. In fluorescence intensity measurements, these two areas give rise to the techniques of fluorescence correlation spectroscopy (FCS)¹⁹ and the photon counting histogram.^{20,21} FRET was first used to study intrachain dynamics by Hass et al.²² It is also possible to examine the relationship between these two sources of fluctuation, resulting in hybrid techniques such as the measurement of burst-integrated fluorescence lifetimes.¹⁸ Other extensions to the basic method include higher-order correlations²³ and the cross-correlations between two fluorescent signals.^{24,25}

Here we examine fluctuations in both time and amplitude, with particular focus on the former, dynamic case.

2. FRET Fluctuation Spectroscopy (FRETfs)

In FRET, the principal property of interest is not fluorescence intensity but the proximity ratio, P

$$P = \frac{I_A}{I_A + I_D} \quad (1)$$

I_A and I_D are the acceptor and donor fluorescence intensities. This ratio is strongly dependent on the separation between the two fluorophores while being independent of diffusional motion.²⁶ If the excitation laser power is kept low, photon-driven processes such as photobleaching can also be neglected, and the proximity ratio becomes independent of the laser intensity.

By looking at temporal correlations in proximity ratio and the distribution of proximity ratio amplitudes, we examine the parameters most strongly related to conformational change. Explicitly, we construct the autocorrelation function of the proximity ratio

$$G_P(\tau) = \frac{\langle \delta P(t) \delta P(t + \tau) \rangle}{\langle P(t) \rangle^2} \quad (2)$$

and a histogram of proximity ratio amplitudes. This proximity ratio distribution is formed in a manner identical to that of the

* Corresponding authors. D.K.: 10012@cam.ac.uk. S.B.: 10013@cam.ac.uk.

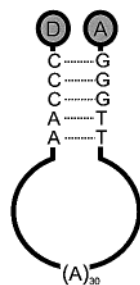


Figure 1. Schematic of the FRET-labeled hairpin loop, Cy5-5'-GGGTT-(A)₃₀-AACCC-3'-TMR. The carboxytetramethylrhodamine (TMR) donor (D) is attached via a modified cytosine six-carbon linker to the 5' terminus of the DNA. The acceptor (A) indodicarbocyanine (Cy5) is attached via a three-carbon linker to the 3' end. When DNA complementary to the loop segment (T₃₀) is added, a duplex is formed, with the arms of the stem sequence free to fluctuate.

single-molecule proximity ratio distribution;^{12,26} however, each data point now comes from the signal of a few molecules rather than one molecule.

3. Experimental Method

A. Materials. Hairpin loops are one of the simplest structures in nucleic acids. The inherent fluctuation present in these systems, from closed to open structures, provide a model case with which to examine biological fluctuation phenomena. On the basis of work by Bonnet et al.,²⁷ we have designed a FRET-labeled DNA hairpin (Cy5-5'-GGGTT-(A)₃₀-AACCC-3'-TMR). A schematic of this structure is presented in Figure 1. The hairpin consists of a 30 base-pair loop segment and a 5 base-pair stem segment. Indodicarbocyanine (Cy5) is joined via a 3-carbon linker to the 5' end of the DNA, and carboxytetramethylrhodamine (TMR) is attached via a modified cytosine residue and a 6-carbon linker to the 3' end of the DNA (Operon Technologies Inc., Alameda, CA). This structure was designed to melt close to room temperature.

B. Experiment. Fluorescence is excited at 514.5 nm, and the signals are detected using a two-channel confocal microscope identical to that used in our previous single-molecule experiments.^{12,28}

Panels a and b of Figure 2 present the single-molecule proximity ratio distributions for a solution of DNA hairpin in MilliQ water and buffer (100 mM NaCl, 2.5 mM Tris-HCl, 250 μ M EDTA), respectively. The data were collected at 0.5 ms resolution with experimental conditions similar to those of our previous work.¹²

Figures 3 and 4 present the results from three fluctuation experiments conducted under identical conditions: constant laser power (100 μ W), hairpin concentration (10 nM), confocal volume (0.3 fl), focal depth above the cover glass (7 μ m), and temperature (18 °C). Figures 3a and 4a correspond to a solution of DNA hairpin in MilliQ water. An identical concentration of DNA was then prepared in TE buffer (100 mM NaCl, 2.5 mM Tris-HCl, 250 μ M EDTA) (Figures 3b and 4b). Finally, a third sample with a large excess of DNA (T₃₀) complementary to the loop segment of hairpin was prepared (10 nM hairpin, 100 mM NaCl, 2.5 mM Tris-HCl, 250 μ M EDTA, 2 μ M T₃₀) (Figures 3c and 4c).

4. Results

A. Single-Molecule Proximity Ratio Distributions. In MilliQ water, the single-molecule proximity ratio distribution shows two distinct components (Figure 2a). In buffer, the high

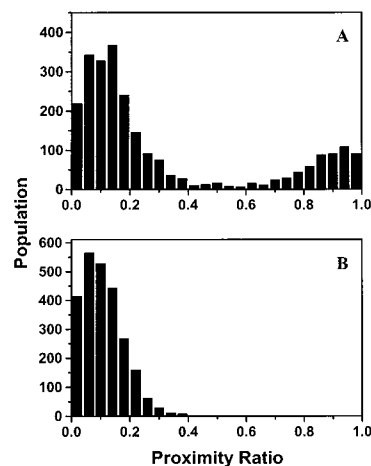


Figure 2. Single-molecule proximity ratio distributions for a 50 pM solution of dual-labeled DNA hairpin-loop (A) in MilliQ water and (B) in a buffer of 100 mM NaCl, 2.5 mM Tris-HCl, and 250 μ M EDTA. A threshold of 10 counts in either donor or acceptor channels is applied to discriminate between the background and the single-molecule signal. The integration time is 0.5 ms, and the excitation laser power is 0.3 mW at 514.5 nm.

proximity ratio component vanishes (Figure 2b). This may be due to either a change in dynamics at a rate faster than the time scale of the measurement (0.5 ms) or a change in the observed static distribution of conformation. As the bulk fluorescence intensity of both TMR and Cy5 do not change significantly from MilliQ to buffer (data not shown), it is likely that a change in dynamics is responsible for the change in the single-molecule proximity ratio distribution. We can begin to investigate this process by decreasing the measurement time.

Measurements at 100 μ s resolution show dynamic information in the trajectories of single molecules through the probe volume (again, data not shown). At this time resolution, single-molecule signal-to-noise levels are low. This means it that is not possible to determine the fluctuation rate by measuring the change in the proximity ratio distribution with binning time. Signal-to-noise levels can be increased by increasing the incident laser intensity, although this is at the expense of introducing additional fluctuations due to fluorophore photophysics.

However, if dynamics are our principal interest, we may concede single-molecule resolution in favor of extracting the dynamic information from the fluctuations of a few molecules (while still retaining a measure of the heterogeneity present).

B. Proximity Ratio Autocorrelation. The graphs in Figure 3 show the proximity ratio autocorrelation for the three samples. Data were collected at 20 μ s resolution with 8 million counting events per channel per curve. The first point in each correlation function is discarded to remove any contribution from cross talk or shot noise. The autocorrelation functions are fitted by a stretched exponential (Kohlrausch–Williams–Watts law)

$$G_p(\tau) = G_p(0) \exp\left[-\left(\frac{\tau}{\tau}\right)^\beta\right] \quad (3)$$

Fitting by double exponentials result in χ^2 values three times larger than those given by stretched exponential decay. Therefore, a stretched exponential provides the more accurate description of the experimental correlation function. The final parameters used in these fits are shown in Table 1.

We assume that the hairpin motion may be described as a two-state conformational fluctuation ($A \rightleftharpoons B$) with static

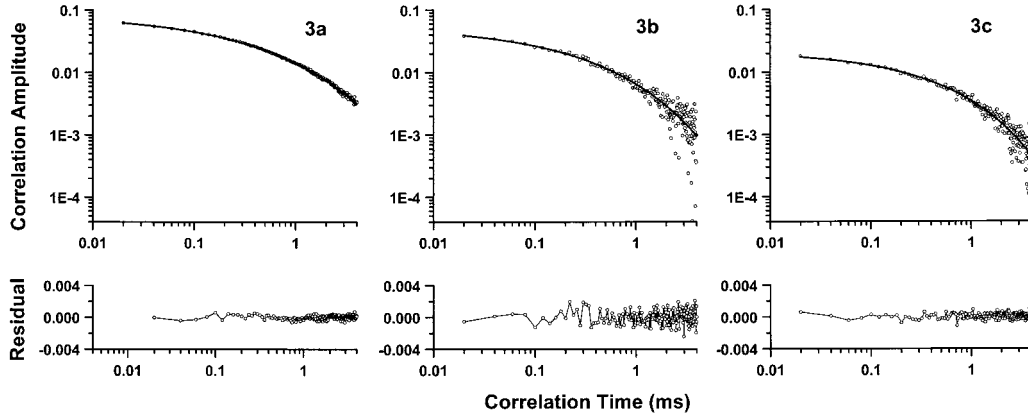


Figure 3. Proximity ratio correlation functions for the FRET-labeled hairpin loop (Cy5-5'-GGGTT-(A)₃₀-AACCC-3'-TMR). (a) DNA hairpin in MilliQ water (20 nM), (b) DNA hairpin in buffer (10 nM hairpin, 100 mM NaCl, 2.5 mM Tris-HCl, and 250 μM EDTA), and (c) hairpin in buffer with an excess (2 μM) of DNA complementary to the loop segment of hairpin (T₃₀) (10 nM hairpin, 100 mM NaCl, 2.5 mM Tris-HCl, and 250 μM EDTA). The three correlation functions are described by a stretched exponential fit, $G_P(\tau) = G_P(0) \exp[-(t/\tau)^\beta]$.

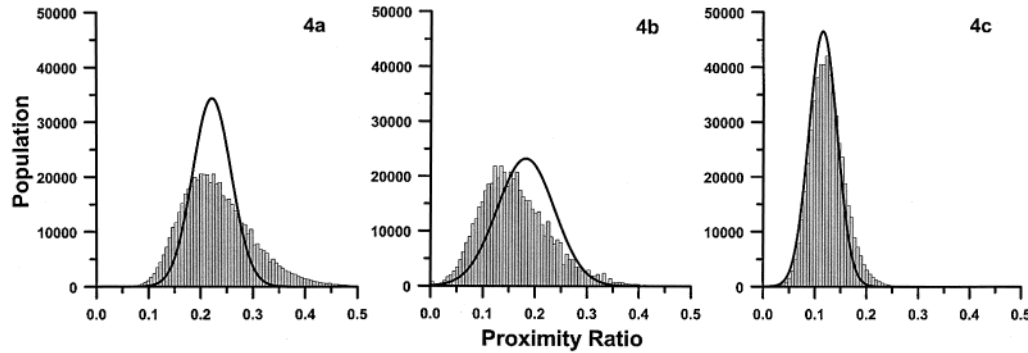


Figure 4. Proximity ratio distributions for the FRET-labeled hairpin-loop (Cy5-5'-GGGTT-(A)₃₀-AACCC-3'-TMR). (a) DNA hairpin in MilliQ water (10 nM), (b) DNA hairpin in buffer (10 nM hairpin, 100 mM NaCl, 2.5 mM Tris-HCl, and 250 μM EDTA), and (c) hairpin in buffer with an excess (2 μM) of DNA complementary to the loop segment of hairpin (T₃₀) (10 nM hairpin, 100 mM NaCl, 2.5 mM Tris-HCl, and 250 μM EDTA). For each case, the fitted function describes the distribution expected from shot-noise alone.

TABLE 1: Stretched Exponential Fits (eq 3) for the Autocorrelation Function of Proximity Ratio in the Conformational Fluctuation of DNA Hairpin Loop under Three Different Conditions^a

| conditions | $G_P(0)$ | τ (ms) | β | $\langle \tau \rangle$ (ms) | anisotropy TMR | Cy5 |
|-------------------------|---------------------|-------------------|-------------------|-----------------------------|-------------------|-------------------|
| MilliQ H ₂ O | 0.0855 ± 0.0006 | 0.267 ± 0.004 | 0.440 ± 0.002 | 0.70 ± 0.02 | 0.095 ± 0.003 | 0.236 ± 0.004 |
| 2.5 mM TE | 0.056 ± 0.002 | 0.19 ± 0.02 | 0.46 ± 0.01 | 0.45 ± 0.08 | 0.088 ± 0.002 | 0.211 ± 0.002 |
| 100 mM NaCl | | | | | | |
| 2.5 mM TE | 0.0218 ± 0.0006 | 0.32 ± 0.02 | 0.54 ± 0.01 | 0.57 ± 0.06 | 0.145 ± 0.001 | 0.234 ± 0.002 |
| 100 mM NaCl | | | | | | |
| 2 μM T ₃₀ | | | | | | |

^a Bulk fluorescence anisotropies are also reported. The uncertainties presented here represent the error in applying a stretched exponential fit and, as such, are an underestimate of the error in the actual experimental variables.

disorder, that there is a large number of fluctuation pathways between states A and B, and that state interconversion is a simple first-order process.^{29–31} For this case, τ corresponds to the effective relaxation time associated with the correlated motion, and β is a stretch parameter describing the heterogeneity of the system. β can vary between 1 (where the system displays normal two-state Arrhenius kinetics, with one discrete energy barrier) and 0 (where there is a continuum of equal energy barriers and the system shows power-law kinetics).

The mean relaxation time $\langle \tau \rangle$ can be related to τ and β by

$$\langle \tau \rangle = \int_0^\infty \exp\left[-\left(\frac{t}{\tau}\right)^\beta\right] dt = \left(\frac{t}{\beta}\right) \Gamma(\beta^{-1}) \quad (4)$$

where $\Gamma(\beta^{-1})$ is a gamma function. For a two-state process, each pathway is characterised by a single relaxation time, which is the inverse of the sum of forward and backward rate constants. $\langle \tau \rangle$ is the mean of all possible relaxation times.

The correlation amplitude $G(0)$ can be approximated by³²

$$G_P(0) = \frac{K}{\langle N \rangle} \left(\frac{1 - Q^2}{1 + QK} \right)^2 \quad (5)$$

where K is the effective equilibrium constant, $\langle N \rangle$ the mean number of fluctuating molecules in the probe volume, and Q the ratio of the proximity ratios for the two states.

C. Proximity Ratio Histogram. For completeness, Figure 4 shows the proximity ratio histograms calculated for the same fluctuation experiment. The histograms focus on the region where a significant population is present ($0 < P < 0.5$). The distributions are calculated at a resolution of 300 μs. This level of binning ensures that the fluctuations are small in comparison with the magnitude of the signal (fluctuations up to three standard deviations from the mean will still give rise to a detectable signal). The background noise is negligible.

In contrast to the single-molecule proximity ratio distributions (Figure 2), the mean proximity ratio from these histograms are in good agreement with the ratio distributions of the bulk. This is due to the need for thresholding in the single-molecule case. However, the distributions from a few molecules (Figure 4a) no longer directly show the two distinct subpopulations observed in the single-molecule distributions for MilliQ water (Figure 2a).

The contribution from shot noise to the distributions in Figure 4 must be considered. The curves displayed in Figure 4 are a simulation based on Poissonally distributed donor and acceptor signals (the details of this simulation are again given in a previous paper¹²). The distributions of proximity ratio seen in Figure 3a,b cannot be accounted for by shot noise alone, indicating that another source of fluctuation must be present. For the case of 3c, where the hairpin-loop is hybridized to the T₃₀ complementary strand, one would expect the DNA to be much more rigid and undergo less fluctuation and, hence, the proximity ratio distribution to more closely reflect the shot-noise limited case. At this time resolution, we can view the addition fluctuation as static conformational heterogeneity.

D. Controls. To relate changes in proximity ratio to changes in molecular conformation, a number of assumptions must be made.^{12,33} In essence, the fluctuations in fluorescence must be dominated by the conformational change of DNA.

TMR anisotropy measurements (Table 1) show that the dye can be approximated as a free rotor under all three experimental conditions, and hence, the fluctuations in proximity ratio are not likely to be due to orientational changes of the fluorophores. These measurements present the static, time-averaged anisotropy. This does not completely rule out the possibility of changes in the rotational freedom of the dye during hairpin fluctuation. However, even if such changes contribute to the observed fluctuations in proximity ratio, it is likely that these fluctuations would also be correlated with the hairpin open to closed transition.

Variations in sample concentration or excitation laser power show no change in proximity ratio correlation time, ruling out the possibility of experimental artifacts or correlations due to photon-driven processes.

The possibility that motion of the fluorophores tethered to their linkers rather than DNA motion gives rise to the observed fluctuations is dismissed using another control. A FRET-labeled DNA 12-mer, hybridized to its complementary strand [12] and under identical buffer conditions, results in almost no detectable correlation in proximity ratio (data not shown). This evidence suggests that there is no significant contribution from the motions of fluorescent labels to the observed fluctuations.

The large changes in proximity ratio from hairpin to duplex support the conclusion that fluctuations in fluorescence, and hence the observed complex dynamics, are dominated by conformational changes of the DNA, not other possible fluctuation phenomena (e.g., DNA–dye interaction). This assumption is also supported by the much slower correlations ($\langle\tau\rangle = 3.4$ ms) observed for a 55% (by weight) glycerol/water mixture. Bulk fluorescence also shows a large decrease in the proximity ratio upon the addition of the complementary strand.

5. Discussion

On the basis of these results, a simple model of hairpin-loop motion is suggested.

In water, there is a lack of counterions to stabilize the hairpin formation.³⁴ In this state, many conformations are possible, and a broad distribution of proximity ratios is seen (greater than

that predicted by the shot noise alone). Correlated motion is observed; however, it is difficult to attribute this to any specific, nonrandom DNA structure. β is also small, describing a broad range of energy barriers.

In buffer solution (Tris-HCl, EDTA, or NaCl), the mean correlation time is reduced, suggesting that the hairpin is now a stable structure and that binding in the stem sequence is the most likely fluctuation phenomenon (i.e., the hairpin open to closed transition). For this case, $\langle\tau\rangle$ represents the average relaxation time for the open-to-closed transition.

When the loop segment is locked by the addition of complementary DNA, the major contribution to the fluctuation is now confined to the motion of the stem arms and not to the open-to-closed transition of the hairpin. This is confirmed by the higher value of stretch parameter β .

As discussed previously, the heterogeneity of the system may be described by the parameter β . For case 2b described in this experiment, β is 0.46; this intermediate value is consistent with a model describing a distribution of barriers, with many potential pathways over a complex energy landscape. The mean lifetimes associated with these three conditions are comparable, but faster than, the ensemble rates of base-pair opening measured by NMR imino proton exchange (<1 to 60 ms).^{35,36}

Stretched exponential kinetics have been observed in protein folding dynamics³⁷ and in the binding of TMR linked to DNA.³⁸ DNA hairpin loops have been examined using a quenching method by Bonnet et al.²⁷ However, limitations in the signal-to-noise ratio in these experiments may affect the fit to the stretched exponential decay. Fluorescence quenching correlation experiments require the use of suitable control samples in order to correct for the diffusion of the fluorescent sample. This diffusional correlation is absent when examining the fluctuations in proximity ratio. The reaction rates measured by Bonnet et al. are similar to the mean relaxation times presented here (approximately 200 μ s, cf. 450 μ s). Their subsequent work on the base-pair opening of double-stranded DNA confirms stretched exponential kinetics.³⁹

By specific incorporation of donor and acceptor fluorophores into the different domains of biomolecules, this technique has the potential of examining the dynamics of many important biological processes. This method is generally applicable to the study of any process involving correlated motion between two sites in the micro to millisecond time regime. For example, FRET fluctuation spectroscopy (FRETfs) may find application in studying ligand binding,⁴⁰ enzyme kinetics,³ and protein folding.⁴¹ In addition, in contrast to more complicated temperature-jump methods, which rely on relaxation from a nonequilibrium state, FRETfs examines kinetics at equilibrium.

The simple experiment reported here demonstrates the potential of fluorescence resonance energy transfer fluctuation spectroscopy (FRETfs) to understand the conformational dynamics of nucleic acids.

Acknowledgment. This work was supported by the Leverhulme Trust (Grant F65OE).

Supporting Information Available: Figure showing proximity ratio correlation functions for two controls.

References and Notes

- (1) Xie, X. S.; Trautman, J. K. *Annu. Rev. Phys. Chem.* **1998**, *49*, 441.
- (2) Nie, S. M.; Zare, R. N. *Annu. Rev. Biophys. Biomol. Struct.* **1997**, *26*, 567.

- (3) Ha, T.; Ting, A. Y.; Liang, J.; Caldwell, W. B.; Deniz, A. A.; Chemla, D. S.; Schultz, P. G.; Weiss, S. *Proc. Natl. Acad. Sci. U.S.A.* **1999**, *96*, 893.
- (4) Weiss, S. *Science* **1999**, *283*, 1676.
- (5) Lu, H. P.; Xun, L.; Xie, X. S. *Science* **1998**, *282*, 1877.
- (6) Dickson, R. M.; Cubitt, A. B.; Tien, R. Y.; Moerner, W. E. *Nature* **1997**, *388*, 355.
- (7) Vale, R. D.; Funatsu, T.; Pierce, D. W.; Romberg, L.; Harada, Y.; Yanagida, T. *Nature* **1996**, *380*, 451.
- (8) Ying, L.; Xie, X. S. *J. Phys. Chem. B* **1998**, *102*, 10399.
- (9) Ha, T.; Zhuang, X.; Kim, H. D.; Orr, J. W.; Williamson, J. R.; Chu, S. *Proc. Natl. Acad. Sci. U.S.A.* **1999**, *96*, 9077.
- (10) Jia, Y.; Talaga, D. S.; Lau, W. L.; Lu, H. S. M.; DeGrado, W. F.; Hochstrasser, R. M. *Chem. Phys.* **1999**, *247*, 69.
- (11) Ha, T.; Enderle, T.; Ogletree, D. F.; Chemla, D. S.; Selvin, P. R.; Weiss, S. *Proc. Natl. Acad. Sci. U.S.A.* **1996**, *93*, 6264.
- (12) Ying, L.; Wallace, M. I.; Balasubramanian, S.; Klenerman, D. *J. Phys. Chem. B* **2000**, *104*, 5171.
- (13) Tamarat P.; Maali A.; Lounis B.; Orrit, M. D. *J. Phys. Chem. A* **2000**, *104*, 1.
- (14) Maiti, S.; Haupts, U.; Webb, W. W. *Proc. Natl. Acad. Sci. U.S.A.* **1997**, *94*, 11753.
- (15) Chen, Y.; Muller, J. D.; Berland, K. M.; Gratton, E. *Methods Enzymol.* **1999**, *19*, 234.
- (16) Eigen, M.; Rigler, R. *Proc. Natl. Acad. Sci. U.S.A.* **1994**, *91*, 5740.
- (17) Edman, L.; Mets, U.; Rigler, R. *Proc. Natl. Acad. Sci. U.S.A.* **1996**, *93*, 6710.
- (18) Eggeling, C.; Fries, J. R.; Brand, L.; Günther, R.; Seidel, C. A. M. *Proc. Natl. Acad. Sci. U.S.A.* **1998**, *95*, 1556.
- (19) Magde, D.; Elson, E.; Webb, W. W. *Phys. Rev. Lett.* **1972**, *29*, 705.
- (20) Chen, Y.; Müller, J. D.; So, P. T. C.; Gratton, E. *Biophys. J.* **1999**, *77*, 553.
- (21) Kask, P.; Kaupo, P.; Fay, N.; Mets, Ü.; Ullmann, D.; Jungmann, J.; Pschorr, J.; Gall, K. *Biophys. J.* **2000**, *78*, 1703.
- (22) Hass, E.; Katchalski-Katzir, E.; Steinberg, I. Z. *Biopolymers* **1978**, *17*, 11.
- (23) Palmer, A. G.; Thompson, N. L. *Biophys. J.* **1987**, *52*, 257.
- (24) Schwille, P.; Meyer-Almes, F. J.; Rigler, R. *Biophys. J.* **1997**, *72*, 1878.
- (25) Kettling, U.; Koltermann, A.; Schwille, P.; Eigen, M. *Proc. Natl. Acad. Sci. U.S.A.* **1998**, *95*, 1416.
- (26) Deniz, A. A.; Dahan, M.; Grunwell, J. R.; Ha, T.; Faulhaber, A. E.; Chemla, D. S.; Weiss, S.; Schultz, P. G. *Proc. Natl. Acad. Sci. U.S.A.* **1999**, *96*, 3670.
- (27) Bonnet, G.; Krichevsky, O.; Libchaber, A. *Proc. Natl. Acad. Sci. U.S.A.* **1998**, *95*, 8602.
- (28) Osborne, M. A.; Balasubramanian, S.; Furey, W. S.; Klenerman, D. *J. Phys. Chem. B* **1998**, *102*, 3160.
- (29) Liebovitch, L. S.; Tóth, T. I. *Bull. Math. Biol.* **1991**, *53*, 443.
- (30) Rabani, E.; Gezelter, J. D.; Berne, B. J. *Phys. Rev. Lett.* **1999**, *82*, 3649.
- (31) Vlad, M. O.; Ross, J.; Huber, D. L. *J. Phys. Chem. B* **1999**, *103*, 1563.
- (32) Elson, E. L.; Magde, D. *Biopolymers* **1974**, *13*, 1.
- (33) Ha, T.; Ting, A. Y.; Liang, J.; Deniz, A. A.; Chemla, D. S.; Schultz, P. G.; Weiss, S. *Chem. Phys.* **1999**, *247*, 107.
- (34) Manning, G. S. *Q. Rev. Biophys.* **1978**, *11*, 179.
- (35) Dornberger, U.; Leijon, M.; Fritzsche, H. J. *Biol. Chem.* **1999**, *274*, 6957.
- (36) Warmlander, S.; Sen, A.; Leijon, M. *Biochemistry* **2000**, *39*, 607.
- (37) Grubele, M. *Annu. Rev. Phys. Chem.* **1999**, *50*, 485.
- (38) Wennmalm, S.; Edman, L.; Rigler, R. *Proc. Natl. Acad. Sci. U.S.A.* **1997**, *94*, 10641.
- (39) Bonnet, G.; Krichevsky, O.; Libchaber, A. *Biophys. J.* **2000**, *78*, A132.
- (40) Zhou, G. C.; Cummings, R.; Li, Y.; Mitra, S.; Wilkinson, H. A.; Elbrecht, A.; Hermes, J. D.; Schaeffer, J. M.; Smith, R. G.; Moller, D. E. *Mol. Endocrinol.* **1998**, *12*, 1594.
- (41) Lillo, M. P.; Beechem, J. M.; Szpikowska, B. K.; Sherman, M. A.; Mas, M. T. *Biochemistry* **1997**, *36*, 11261.